

Measurement and Correlation of Vapor–Liquid Equilibria for the 2-Propanol + *n*-Hexane System near the Critical Region

Jungha Seo,[†] Jongcheon Lee,[‡] and Hwayong Kim^{*,§}

Korea Institute of Industrial Technology Evaluation & Planning, Kotech 8th floor, 701-7, Yeoksam-Dong, Gangnam-Gu, Seoul 135-080, Korea, and Institute of Chemical Processes and School of Chemical Engineering, Seoul National University, SAN 56-1, Shilim-Dong, Kwanak-gu, Seoul 151-744, Korea

Isothermal vapor–liquid equilibrium data of the 2-propanol + *n*-hexane system were measured at near-critical temperatures to be compared with similar data for the ethanol + *n*-hexane and methanol + *n*-hexane systems. The critical pressure was determined from the critical opalescence of the mixtures. A circulating type apparatus with a view cell was used. These mixtures are highly nonideal due to the association of the alcohol. The data could be correlated with sufficient accuracy by using the Peng–Robinson–Stryjek–Vera equation of state with Wong–Sandler mixing rules.

Introduction

In the near-critical region, vapor–liquid equilibrium (VLE) measurements for polar and nonpolar mixtures are necessary because the properties of such mixtures cannot be predicted from corresponding pure-component values. Therefore, vapor–liquid equilibrium data for these mixtures are essential to develop new thermodynamic models and to design and operate new processes. Seo et al.¹ reported VLE data for the systems ethanol + *n*-hexane by the circulating method, and de Loos et al.² reported VLE data for the system methanol + *n*-hexane by the static nonanalytic method. In this work, we measured the equilibrium pressure (*P*), temperature (*T*), liquid-phase composition (*x*), and vapor-phase composition (*y*) for the 2-propanol and *n*-hexane system.

Experimental Section

Materials. 2-Propanol was supplied by Fluka with a minimum purity of 99.9%. *n*-Hexane was supplied by Fluka with a minimum purity of 99.5% (GC) and stored over a molecular sieve. To degas the chemicals, we stored the chemicals at a slightly higher pressure than the vapor pressure of each chemical.

Apparatus and Procedures. Details of this apparatus are given in our previous work.^{1,3} The equilibrium cell features quartz sight glass on both faces and two circulation magnetic pumps to promote equilibrium. The forced convection oven keeps the temperature of the cell and pumps uniform. The accuracy of the temperature measuring system is ±0.03 K in the range of (373 to 673) K according to the manufacturer's specifications, and the accuracy of the pressure transducer was expected to be ±0.1% according to specifications but was actually ±0.05% after a calibration by the Korea Testing Laboratory.

The quartz sight glasses require specially designed, high-pressure seals for operation at 45 bar and 230 °C. A schematic diagram of the sealing mechanism is shown in

Figure 1. A stainless steel faceplate is bolted to the cell body with each bolt having an applied torque of 16.2 N·m. The faceplate forces the quartz window against a Teflon vortex gasket to give a uniform seal between the gasket and the window and between the gasket and the cell body. A type 316 stainless steel antiextrusion ring prevents excessive extrusion and compression of the gasket. Stainless steel spring washers compensate for thermal expansion of the bolts at elevated temperatures.

The samples were analyzed by gas chromatography (GC) on line. TCD and Porapak Q packing columns were used. The manifold valves with two needle type stems were used as sampling valves. The inner volume of each valve was large, about 0.05 mL. Thus, the GC columns were specially manufactured with 0.95 cm o.d. × 85 cm length tube for the application to the large amount of sample. A total mass of 13.5 g of packing material was used in each column.

Results and Discussion

Thermodynamic Model. For the correlation of the experimental data, we used the Peng–Robinson–Stryjek–Vera (PRSV) equation of state⁴ with the reformulated Wong–Sandler⁵ mixing rules where the composition-independent cross second virial coefficient is given by

$$\left(b - \frac{a}{RT}\right)_{ij} = \frac{b_i + b_j}{2} - \frac{\sqrt{a_i a_j}}{RT}(1 - k_{ij}) \quad (1)$$

This reformulated equation was proposed by Orbey and Sandler to recover the classical mixing rules when used with the modified nonrandom two-liquid (NRTL) model by Huron and Vidal.⁶ However, A_{∞}^E was chosen from the original NRTL model⁷ as follows:

$$A_{\infty}^E = \sum_{i=1}^n x_i \frac{RT \sum_{j=1}^n x_j G_{ji} \tau_{ji}}{\sum_{k=1}^n x_k G_{ki}} \quad \text{with } G_{ji} = \exp(-\alpha_{ji} \tau_{ji}) \quad (2)$$

where

* Corresponding author. E-mail: hwayongk@snu.ac.kr. Tel: +82-2-880-7406. Fax: +82-2-888-6695.

[†] Korea Institute of Industrial Technology Evaluation & Planning.

[‡] Institute of Chemical Processes, Seoul National University.

[§] School of Chemical Engineering, Seoul National University.

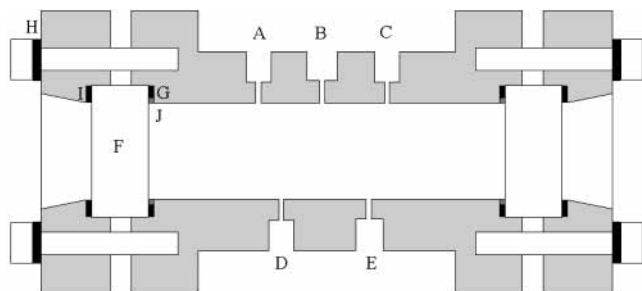


Figure 1. Schematic diagram of the mechanism for sealing the windows of the equilibrium cell: A, thermostat; B,E, liquid circulation connection; C,D, vapor circulation connection; F, quartz sight glass; G, vortex gasket; H, SUS spring washer; I, graphite cushion; J, antiextrusion ring.

$$\tau_{ji} = \frac{c_{ji}}{RT}$$

We also applied the modified Soave–Redlich–Kwong (SRK) equation of state⁸ with the MHV2⁹ mixing rules resulting in the fugacity coefficient,

$$\ln \phi_i = \ln \left[\frac{RT}{P(v-b)} \right] + \left[\frac{1}{v-b} - \frac{a/bRT}{v+b} \right] b_{ii} - \left(\frac{\partial(na/bRT)}{\partial n_i} \right)_{T,n_j} \ln \left[\frac{v+b}{v} \right] \quad (3)$$

with

$$\left(q_1 + 2q_2 \frac{a}{bRT} \right) \frac{\partial(na/bRT)}{\partial n_i} = q_1 \frac{a_{ii}}{b_{ii}RT} + q_2 \left[\left(\frac{a}{bRT} \right)^2 + \left(\frac{a_{ii}}{b_{ii}RT} \right)^2 \right] + \ln \gamma_i + \ln \frac{b}{b_{ii}} + \frac{b_{ii}}{b} - 1 \quad (4)$$

where the molar excess Gibbs energy G_v^E for the activity coefficient, γ_i , was chosen from the original NRTL model.⁷

Vapor–Liquid Equilibrium Measurements. The isothermal vapor–liquid measurements were determined at (483.15, 493.15, and 503.15) K for *n*-hexane and 2-propanol. The experimental data are listed in Table 1. When the Wong–Sandler (WS) mixing rule was applied, the nonrandomness parameter, α , was fixed as 0.1, and three parameters, k_{12} , τ_{12} , and τ_{21} , were fitted. The objective function for evaluating the parameters is given by

$$SQ = SQP + SQY = \sum_{N=1}^{N_T} \left(\frac{P_{\text{cal}} - P_{\text{exp}}}{P_{\text{exp}}} \right)^2 + \sum_{N=1}^{N_T} (y_{\text{cal}} - y_{\text{exp}})^2 \quad (5)$$

The percentage root-mean-squared relative deviations between the measured and calculated pressure, $100(SQP/N_T)^{1/2}$, the root-mean-squared deviations of vapor composition of component 1, $100(SQY/N_T)^{1/2}$, and the values of k_{12} , τ_{12} , and τ_{21} are listed in Table 2. The maximum deviation of pressure does not exceed 0.54%. The comparison between the calculated and the experimental values is presented in Figure 2. In the case of the MHV2 mixing rule, three parameters, α , τ_{12} , and τ_{21} , were fitted only at 483.15 K and the values are -0.008906 , -1.613 , and 2.425 , respectively. In this case, $100(SQP/N_T)^{1/2}$ is 0.75%, and the deviation of pressure is larger than the 0.40% with the Wong–Sandler model. The correlation results of this

Table 1. Experimental VLE Data for the *n*-Hexane (1) + 2-Propanol (2) Systems and Calculation Results

<i>T</i> /K	P_{exp} /bar	P_{cal} /bar	$x_{1,\text{exp}}$	$y_{1,\text{exp}}$	$y_{1,\text{cal}}$	
503.15	43.62	43.71	0.000	0.000	0.000	
	44.20	44.20	0.022	0.027	0.024	
	44.70	44.70	0.048	0.055	0.050	
	45.46		0.087	0.091		
	45.46 ^a		0.099	0.099		
	32.14 ^a		0.906	0.906		
	32.00		0.912	0.908		
	31.43		0.928	0.921		
	30.62	30.62	0.947	0.941	0.943	
	29.45	29.46	0.973	0.970	0.968	
	28.38	28.44	1.000	1.000	1.000	
	493.15	36.77	36.90	0.000	0.000	0.000
		37.60	37.69	0.040	0.045	0.047
		38.10	38.16	0.068	0.079	0.077
38.78		38.80	0.116	0.123	0.125	
39.32		39.28	0.166	0.171	0.172	
39.61		39.59	0.218	0.222	0.220	
39.85			0.287	0.281		
39.78			0.350	0.342		
39.58			0.379	0.371		
39.32			0.418	0.409		
39.21 ^a			0.427	0.427		
37.26 ^a			0.558	0.558		
37.12			0.566	0.565		
36.71			0.590	0.584		
34.68		0.685	0.667			
32.39		0.772	0.748			
30.50	30.48	0.837	0.815	0.815		
28.47	28.46	0.897	0.878	0.870		
26.80	27.16	0.935	0.924	0.912		
24.53	24.67	1.000	1.000	1.000		
483.15	30.81	30.90	0.000	0.000	0.000	
	31.41	31.48	0.029	0.042	0.037	
	32.22	32.28	0.078	0.092	0.093	
	33.21	33.24	0.165	0.178	0.180	
	33.59	33.64	0.234	0.241	0.242	
	33.75	33.77	0.295	0.301	0.296	
	33.76	33.75	0.328	0.327	0.325	
	33.54	33.57	0.387	0.375	0.377	
	33.06	33.02	0.466	0.444	0.449	
	32.74	32.69	0.499	0.479	0.479	
	31.94	31.86	0.565	0.534	0.539	
	31.04	30.95	0.624	0.591	0.591	
	28.62	28.56	0.748	0.704	0.700	
	27.43	27.32	0.802	0.758	0.750	
24.31	24.55	0.904	0.878	0.859		
21.09	21.29	1.000	1.000	1.000		

^a Critical pressure.

Table 2. Results of the VLE Correlation for the *n*-Hexane (1) + 2-Propanol (2) System by the PRSV Equation of State and WS Mixing Rule

<i>T</i> /K	k_{12}	τ_{12}	τ_{21}	$100(SQP/N_T)^{1/2}/\%$	$(SQY/N_T)^{1/2}$
503.15	0.076 20	0.1686	1.109	0.12	0.003
493.15	0.077 32	1.122	0.2543	0.49	0.005
483.15	0.086 69	1.122	0.2543	0.40	0.006

system are very accurate in the subcritical region. However, the problem remains for an accurate representation in the near-critical region, as indicated by Sandler.¹⁰

Critical points were also determined from the critical opalescence of the mixture. The critical mole fractions of *n*-hexane were found to be 0.099 and 0.906 (at 503.15 K) and 0.427 and 0.558 (at 493.15 K). In Figure 3, the *PT* diagram of critical locus indicates that two critical points exist at (503.15 and 493.15) K. The azeotropic pressure of 39.85 bar at 493.15 K in Figure 2 and Figure 3 is higher than the critical pressure, 39.21 bar. In addition, the critical loci by Seo et al. and by de Loos et al. are also given for comparison with this work in Figure 4.

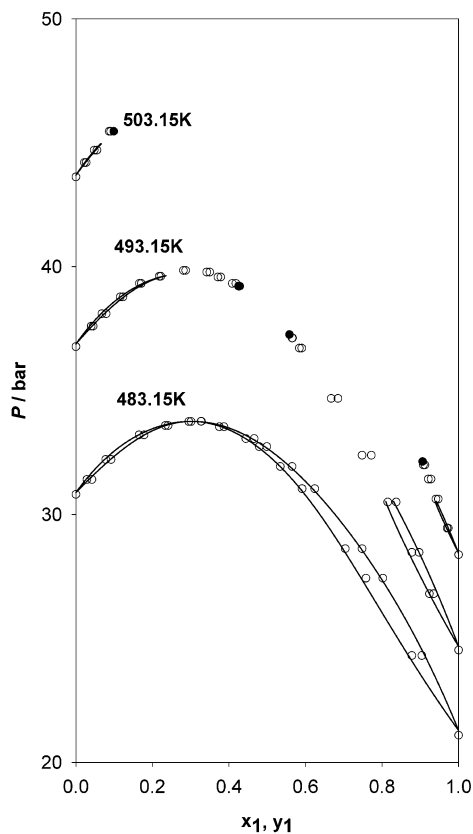


Figure 2. Correlation of the *n*-hexane (1) and 2-propanol (2) system: ●, critical points.

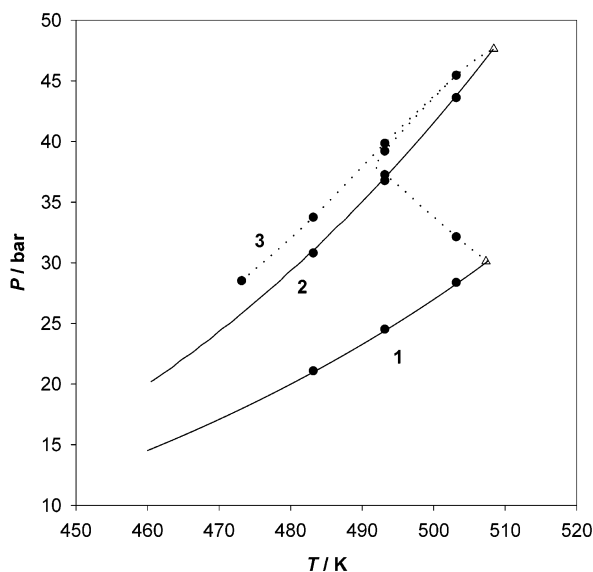


Figure 3. Critical locus and pure vapor pressure curve for *n*-hexane (1), 2-propanol (2), and an azeotropic mixture (3): ●, this work; —, property data bank by Reid et al. (ref 12); △, critical points of pure components from the data bank by Reid et al.; ···, interpolation curves.

For the critical point calculation, we applied the method reported by Castier and Sandler.¹¹ P - T - x - y data at a subcritical temperature, 483.15 K, were used to estimate three parameters in the NRTL model: α , c_{12}/R , and c_{21}/R . Table 3 presents the parameters used for the critical point calculations of each system reported herein. When α is fixed as 0.1, the calculation result underestimates the critical temperatures as shown in Figure 5. This offers a good explanation for the inaccuracy of the correlation of VLE in

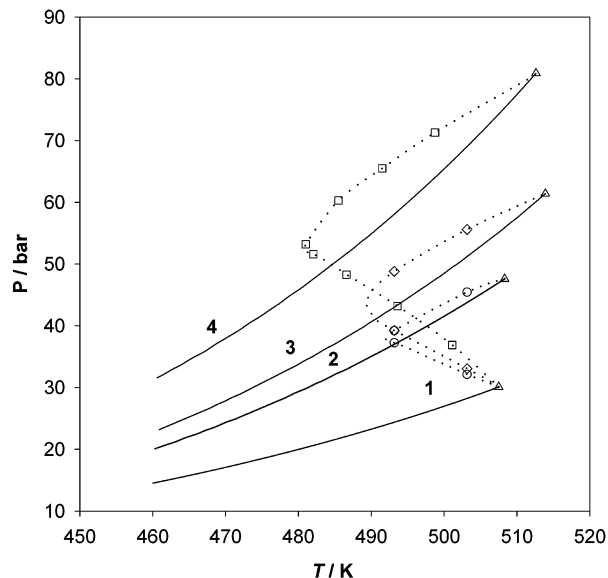


Figure 4. Critical locus and pure vapor pressure curves for *n*-hexane (1), 2-propanol (2), ethanol (3), and methanol (4): ○, this work; ◇, Seo et al. (ref 1); □, de Loos et al. (ref 2); —, property data bank by Reid et al. (ref 12); △, critical points of pure components from the data bank by Reid et al.; ···, interpolation curve.

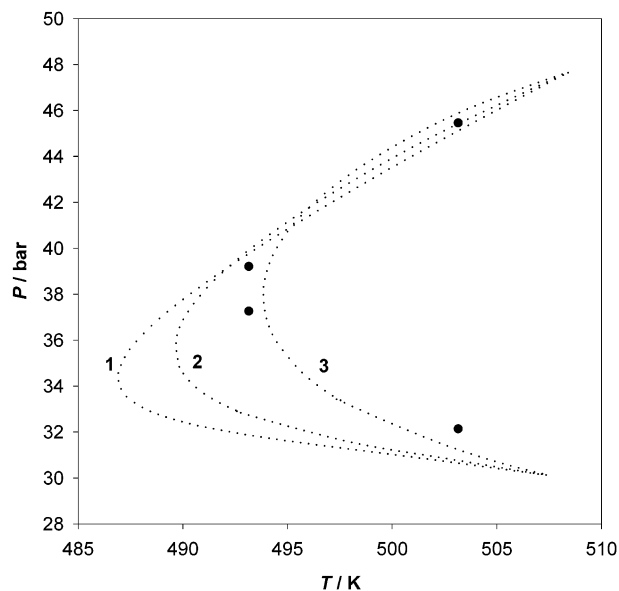


Figure 5. Critical curve of the system *n*-hexane + 2-propanol; pressure-temperature projection: 1, predicted with α fixed as 0.1; 2, predicted with α fixed as 0.9; 3, predicted with α fixed as 1.2; ●, critical points.

Table 3. VLE Parameters for the System 2-Propanol + *n*-Hexane at 483.15 K

T/K	α	c_{12}/R	c_{21}/R	k_{12}	$100(\text{SQP}/N_T)^{1/2}/\%$
483.15	0.1	542.1	122.9	0.08669	0.40
	0.9	542.4	400.4	0.1227	0.63
	1.2	528.8	320.7	0.1772	0.64

the near-critical region, shown in Figure 2. If the parameter α is chosen to be 1.2 in order to fit the critical locus, a better VLE correlation could be the result. However, the value 1.2 is so large that it cannot be generally acceptable as an NRTL parameter.

Conclusions

Isothermal vapor-liquid equilibria for *n*-hexane + 2-propanol were obtained at near-critical temperatures. The

PRSV equation of state and Wong–Sandler mixing rules produced good correlation parameters of the data in the subcritical region. However, more improvements are required to give an accurate correlation in the near-critical region.

Acknowledgment

We thank Drs. Castier and Sandler for providing the critical point calculation program.

List of Symbols

\bar{A}	E_{∞} molar excess free energy at high density
a	parameter of the equation of state
b	parameter of the equation of state
\bar{G}	E_{γ} molar excess Gibbs energy
k_{ij}	binary interaction parameter
n	number of moles
N_T	number of data points
P	pressure
q_1, q_2	mixing rule constants
R	universal gas constant
SQP	mean squared relative deviation of pressure
SQY	squared and summarized deviation of vapor
T	temperature
v	molar volume
x	mole fraction of liquid phase
y	mole fraction of vapor phase

Greek Letters

α	nonrandomness parameter
ϕ	fugacity coefficient
γ	activity coefficient
τ	parameter in the mixing rule

Subscripts

c	critical
cal	calculated

exp	experimental
r	reduced

Literature Cited

- (1) Seo, J.; Lee, J.; Kim, H. Isothermal vapor–liquid equilibria for the system ethanol and *n*-hexane in the near critical region. *Fluid Phase Equilib.* **2001**, *182*, 199–207.
- (2) De Loos, Th. W.; Poot, W.; de Swaan Arons, J. Vapour–liquid equilibria and critical phenomena in methanol + *n*-alkane systems. *Fluid Phase Equilib.* **1988**, *42*, 209–227.
- (3) Seo, J.; Lee, J.; Kim, H. Isothermal vapor–liquid equilibria for ethanol and *n*-pentane system at the near critical region. *Fluid Phase Equilib.* **2000**, *172*, 211–219.
- (4) Stryjek, R.; Vera, J. H. PRSV: An improved Peng–Robinson equation of state for pure compounds and mixtures. *Can. J. Chem. Eng.* **1986**, *64*, 323–333.
- (5) Orbey, H.; Sandler, S. I. Reformulation of Wong–Sandler mixing rule for cubic equation of state. *AIChE J.* **1995**, *41*, 683–690.
- (6) Huron, M. H.; Vidal, J. New mixing rules in a simple equation of state for representing vapor–liquid equilibria of strongly nonideal mixtures. *Fluid Phase Equilib.* **1979**, *3*, 255–271.
- (7) Renon, H.; Prausnitz, J. M. Local compositions in thermodynamic excess functions for liquid mixtures. *AIChE J.* **1968**, *14*, 135–144.
- (8) Sandarasi, J. A.; Kidnay, A. J.; Jessavage, V. F. Compilation of parameters for a polar fluid Soave–Redlich–Kwong equation of state. *Ind. Eng. Chem. Process Des. Dev.* **1986**, *25*, 957–963.
- (9) Dahl, S.; Michelsen, M. L. High-pressure vapor–liquid equilibrium with a UNIFAC-based equation of state. *AIChE J.* **1990**, *36*, 1829–1836.
- (10) Sandler, S. I. *Models for Thermodynamic and Phase Equilibria Calculations*; Marcel Dekker: New York, 1994; p 114.
- (11) Castier, M.; Sandler, S. I. Critical points with the Wong–Sandler mixing rule –II. Calculations with a modified Peng–Robinson equation of state. *Chem. Eng. Sci.* **1997**, *52*, 3579–3588.
- (12) Reid, R. C.; Prausnitz, J. M.; Poling, B. E. *The Properties of Gases & Liquids*, 4th ed.; McGraw-Hill: Singapore, 1988; pp 656–732.

Received for review August 27, 2002. Accepted April 10, 2003. This work was supported by the BK21 project of the Ministry of Education and the National Research Laboratory (NRL) Program of the Korea Institute of Science & Technology Evaluation and Planning.

JE025604S